Pietro Valdastri
e-mail: pietro@sssup.it

Keith Houston

Arianna Menciassi

Paolo Dario

CRIM Lab,
Scuola Superiore Sant'Anna,
56100, Pisa, Italy

Arne Sieber
Profactor Research and Solutions GmbH,
A-2444, Seibersdorf, Austria

Masaru Yanagihara

Masakatsu Fujie

Waseda University,
169–8555, Tokyo, Japan

Miniaturized Cutting Tool With Triaxial Force Sensing Capabilities for Minimally Invasive Surgery

This paper reports a miniaturized triaxial force sensorized cutting tool for minimally invasive robotic surgery. This device exploits a silicon-based microelectromechanical system triaxial force sensor that acts as the core component of the system. The outer diameter of the proposed device is less than 3 mm, *thus enabling the insertion through a 9 French catheter guide. Characterization tests are performed for both normal and tangential loadings. A linear transformation relating the sensor output to the external applied force is introduced in order to have a triaxial force output in real time. Normal force resolution is* 8.2 bits *over a force range between* 0 N *and* 30 N, *while tangential resolution is 7 bits over a range of* 5 N. *Force signals with frequencies up to* 250 Hz *can successfully be detected, enabling haptic feedback and tissue mechanical properties investigation. Preliminary ex vivo muscular tissue cutting experiments are introduced and discussed in order to evaluate the device overall performances.*
[DOI: 10.1115/1.2778700]

1 Introduction

In the past few decades, a large amount of microelectromechanical systems (MEMSs) have been developed in order to satisfy different needs in biomedical, applications. Nowadays, one of the most important challenges is to integrate these MEMSs into usable devices that should be able to fill the gap between Micro-System Technology (MST) and end users. Taking advantage of the limited dimensions of MEMS, new small and "smart" surgical tools can be designed and implemented in order to enhance the outcomes of minimally invasive surgery (MIS) procedures [1].

The development of systems for endoscopic surgery originated 40 years ago with the research on instrumented catheters [2]. The advantage offered by catheters is to introduce sensors onto the tip of an elongated, small diameter device able to reach the most remote regions of the human body.

The integration of MEMS sensors into catheter tips has been mainly pursued for diagnostic purposes, e.g., pressure measurement inside blood vessels. Silicon micromachining has been used [3] in order to develop a fiber-optic pressure sensor with an outer diameter of 0.36 mm. Other examples, commercially available, are produced by several biomedical companies [4,5]. More recently, catheters have also been used for therapeutic goals: Some of them can integrate deployable stents to repair aneurysms or deployable superelastic balloons for angioplasty. The advancement of the catheter is performed by the medical doctor, who must insert the device by turning and selecting the right branch to explore or to treat. This operation requires extensive training and understanding of the environment. Usually, the medical doctor relies only on the force feedback that his/her hands receive and on visual feedback provided by intraoperative imaging. Tactile sensing is transferred from the tip of the catheter through itself and, if the device is not stiff enough, it is almost impossible to detect the condition of its tip without sensing devices located in the distal end of the catheter. Several solutions that take advantage of MEMS sensors have been presented to overcome this problem. An interesting example [6] is a compound cavity tactile sensor that uses a surface-emitting laser to detect frontal pushing force. In a similar solution [7], a silicon micromachined pressure sensor is embedded in the catheter tip by using a silicone gel. Both these examples have the limitation of a monoaxial force sensing, i.e., if the angle between the catheter tip and the lumen wall is lower than 90 deg, then the pushing force could be dramatically underestimated and severe damaging of tissues can occur.

A more advanced solution for catheter insertion is given by active guide wires with bending capabilities [8]. A similar version which embeds contact sensors and a closed loop control movement is presented by Olympus [9]. Even if the authors use three contact sensors, placed around the tip at 120 deg to each other, the detection of the contact angle is still not completely reliable.

Another important biomedical field that can take advantages of triaxial force information acquired using miniaturized smart tools is MIS. Surgical tools for this kind of applications already exist [10], but the technology used for sensing consists of traditional metallic structures with commercial strain gauges, and therefore these systems are difficult to be scaled down to very small dimensions.

Force feedback plays a fundamental role in robotic MIS, also known as MIRS. With the recent development of robotic fixtures, more attention has usually been devoted to improve actuation of tools and to maximize their degrees of freedom [11]. On the other hand, the role of force feedback in surgery is well assessed [12], and some examples [13–16] of microinstruments embedding sensors in order to drive the force feedback of haptic displays have been developed so far. A MEMS-based tip force sensor for triaxial force feedback in robot assisted manipulation can significantly improve the procedure outcomes [17]. Good sensitivity and linearity are reported in this work, even if the final overall size of this sensor (diameter of 12.5 mm) and the lack of scalability make this device inadequate for endoluminal interventions. A scalpel embedding a force sensor for MIS with a diameter of 10 mm has

Submitted to ASME for publication in the JOURNAL OF MEDICAL DEVICES. Manuscript received July 19, 2006; final manuscript received August 8, 2007. Review conducted by Gerald E. Miller. Paper presented at the Eight Biennial ASME Conference on Engineering Systems Design and Analysis (ESDA2006), Torino, Italy, July 4–7, 2006.

also been developed [10] to provide the surgeon with direct haptic information. The sensor, consisting of a metallic structure with commercial strain gauges, is placed directly behind the blade and can measure forces up to 20 N. A complete setup for measuring cutting forces of a surgical knife on liver tissue is reported in literature [18,19]. The force data are acquired by a commercial multiaxial load cell and are used to build a local finite element model of blade-tissue interactions. Modeling of deformable tissues is critical for providing accurate haptic feedback to the surgeon in common surgical tasks such as grasping, cutting, and dissection. A novel haptic model for a scalpel and its interactions with 3D soft tissue has been developed by Bielser and Gross [20]. This model is based on tetrahedral volume meshes and provides more topological flexibility if compared to standard frameworks.

Preliminary results concerning the integration at the tip of a surgical cutting instrument of a silicon-based triaxial force sensor [21,22] have been reported by the authors [23]. The developed device has an outer diameter of 7.4 mm that makes it unsuitable for applications where small dimensions are required, such as endoluminal interventions. In the present paper, a triaxial force sensorized cutting tool, having a similar design to author's previous work [23], but with an outer diameter lower than 3 mm, is designed, modeled, fabricated, and tested in cutting tasks. This device enables the detection of cutting forces without visual feedback in endoluminal surgery and force control operation in MIRS. This device can also be used to recover data for haptic recording of tissue properties and for modeling local interactions between the blade and soft tissues in cutting tasks [24]. The same kind of design, fabrication, and calibration results applies for the embedding of the sensor inside the tip of a 9 French catheter, in order to address the catheter insertion problem, or as a distal part of a miniaturized robotic fixture that must be used for triaxial force sensing. For these applications, the blade placed on the device tip must be substituted with a suitable probing end. A proper tailoring of the packaging parameters is also needed in order to meet the specific application requirements in terms of size, weight, range of forces, and signal bandwidth.

The design, fabrication, and signal conditioning are addressed in Sec. 2. The device calibration is described in Sec. 3. Preliminary ex vivo cutting experiments of muscular tissues are reported in Sec. 4. Finally, conclusions and future works are illustrated in Sec. 5.

2 System Design And Fabrication

2.1 System Design. The main issue to consider during the design phase of the miniaturized cutting tool is to increase the robustness of the silicon triaxial force sensor through a proper packaging that can be adequate for the target application. The overloading limits for the bare MEMS sensor are 3 N for normal loadings and 0.5 N for tangential loadings [22]. In order to increase these limits, a compliant polyurethane filling was selected to embed the force sensor. The polymer, penetrating inside the MEMS cavities, acts as a mechanical soft stop, thus avoiding the breaking of the silicon device, represented in Fig. 4(a). In addition to this, the packaging structure must transmit the force to the MEMS sensor in a symmetrical way, in order to maintain the information about the stimulus orientation. Thus, a nylon ball was selected as mechanical interface between the blade and the polyurethane filling that embeds the sensor, as represented in Fig. 1. A sharp ruby blade was attached to the flat surface of the nylon ball. The blade is 5 mm long, 1.5 mm wide, and 500 μm thick.

All the selected materials are biocompatible and the polyurethane filling has also the function of sealing the inner space of the device, thus avoiding interactions between the electronics and the physiological environment.

Thanks to the process described in the next subsection, it was possible to achieve an outer diameter less than 3 mm (specifically 2.95 mm), so that the device can be introduced into the human body through a 9 French catheter guide. The nylon ball has a

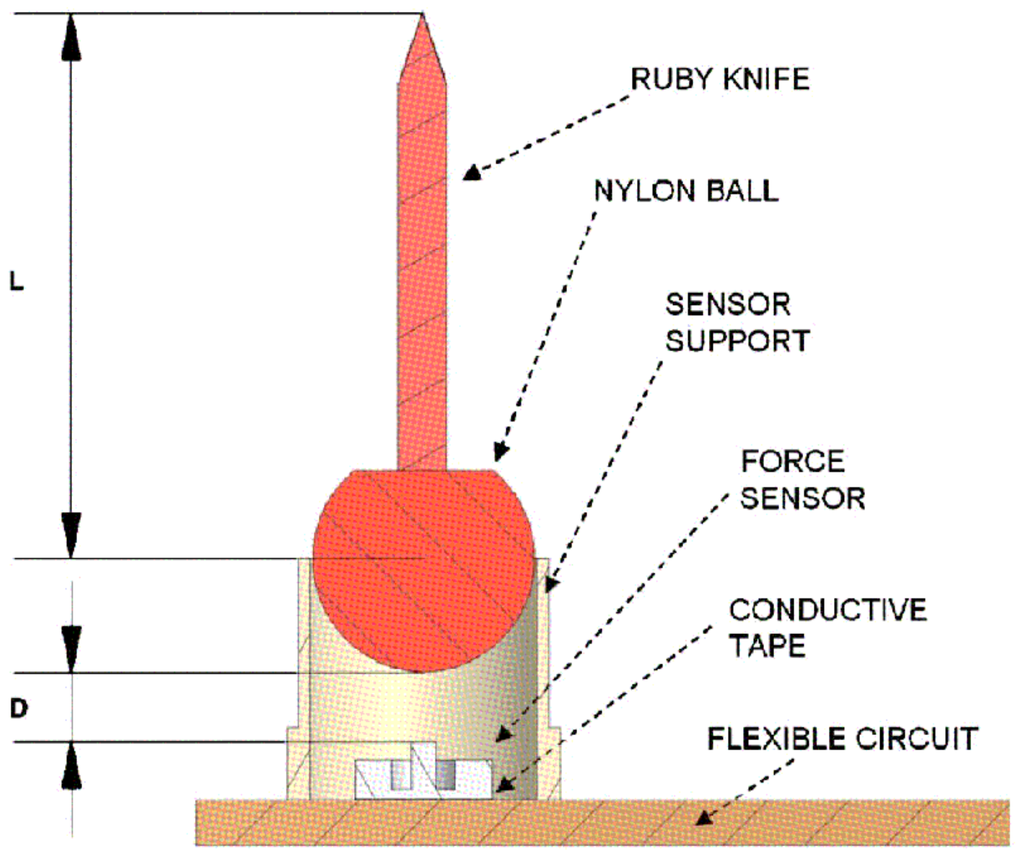

Fig. 1 Cross section of the device

diameter of 2.5 mm and the length L, reported in Fig. 1, is 6 mm.

The polyurethane filling has the drawback of decreasing the device sensitivity. Thus, a trade-off between device robustness and sensitivity must be found through a proper tailoring of the distance D (Fig. 1) that separates the MEMS sensor tip from the lower surface of the nylon ball and defines the polymer volume. For this reason, a set of finite element simulations was carried out for normal loading forces. The software used was FEMLAB 3.0 and a 3D solid linear element model was used. The polyurethane was assumed to be a purely elastic material and the silicon sensor material was assumed to be isotropic. The model agreed well with experimental calibration results reported later in the paper. Thus, it was decided to perform further simulations to determine the effect of changes in D. From these simulations, reported in Fig. 2, it was observed that when D was reduced from 1 mm to 0 mm, the fractional change in resistance, that is proportional to the sensor output voltage, for a 1 N simulated normal load, was more than doubled. When D was increased from 1 mm to 2 mm, the fractional change in resistance had only a 30% reduction. It can be inferred that the relationship between D and the force necessary to produce fracture of the silicon sensor at its weakest point would mirror this pattern. When D is reduced from 2 mm to 0 mm, the maximum stress increases by over a factor of 3.

Figure 3(a) shows the quarter solid model of the device with D of 1 mm for a 1 N normal loading, while Fig. 3(b) is the boundary plot of total displacement. From these pictures, it is possible to observe that a large portion of the force is absorbed in the polyurethane between the sphere and the device outer walls, where a large amount of the force is stored as shear strain energy. This

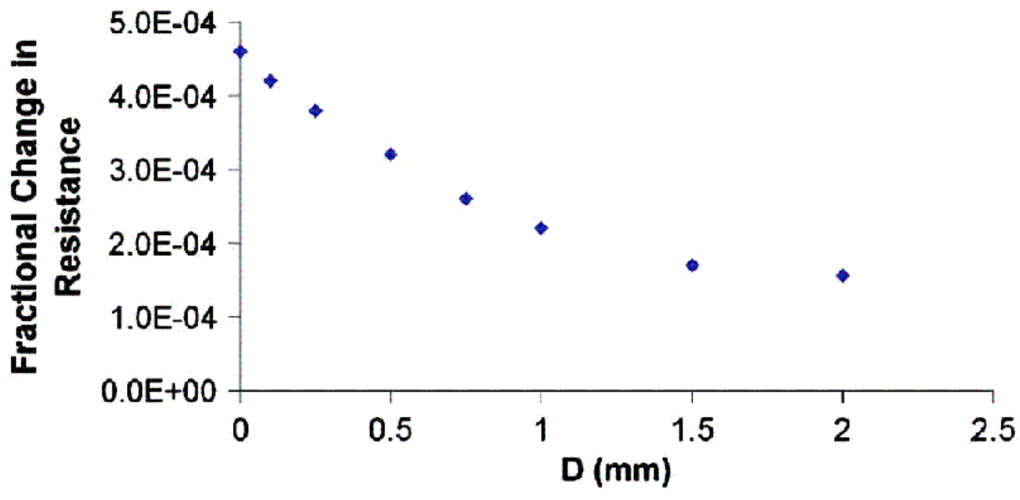

Fig. 2 Simulated fractional change in resistance for a 1 N normal loading with different *D* values

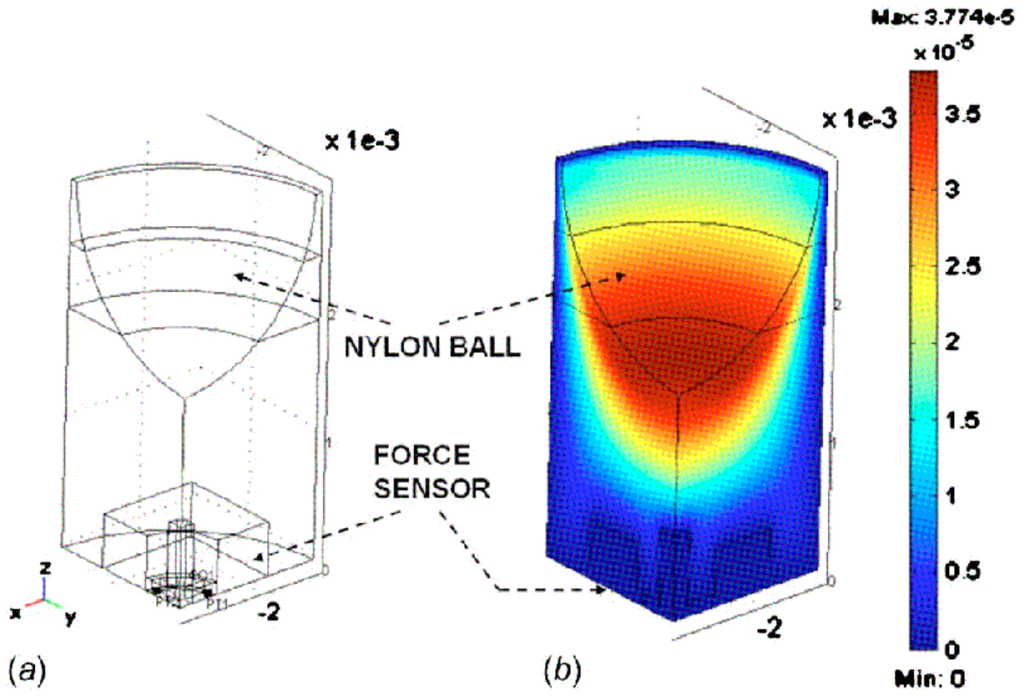

Fig. 3 (*a*) Quarter solid model and (*b*) boundary plot of total displacement of the device for a 1 N normal loading

explains why there is not such a significant increase of the fractional change in resistance from $D=1$ mm to $D=2$ mm and also why the sensor becomes more robust once embedded into the polymer.

From these considerations and from some preliminary experimental results, $D=1$ mm was selected as design parameter, in order both to sense forces in a range typical for tissue cutting [18] and to be robust enough to withstand occasional overloading.

2.2 System Fabrication. In the 7.4 mm diameter cutting tool [23], the sensing element, represented in Fig. 4(*a*), was the triaxial force sensor [21] fixed by conductive glue to a silicon support (2.3×2.3 mm). This support was then glued onto a flexible circuit and its pads were wire bonded to copper tracks. This operation required additional space, thus obtaining a final diameter of 7.4 mm for the device.

The main innovation that allowed to reduce the outer diameter from 7.4 mm to 2.95 mm was mounting the sensor directly onto the flexible circuit, obtained from LF9150R Pyralux (DuPont, Wilmington, DE). In order to achieve this task, the nine contacts (diameter of 200 μm) of the sensor (two contacts for each piezoresistor, as represented in Fig. 4(*b*), and one for the bulk) must be connected to copper pads on the flexible circuit and a good and reliable mechanical bonding must be established.

To find the most suitable bonding method, different kinds of techniques were investigated. A microassembly station was set up consisting of a hot plate (25–300 °C), mounted on an x-y manual micrometric translation stage (M-105.10, PI, Germany), and a suction gripper (for holding and placing the sensor), mounted on a servocontrolled nanometric translation stage, with a dc servomotor (111-1DG, PI, Germany) for fine normal direction movements. For dispensing conductive glue or solder paste, a microdispenser (1000XL, EFD, Burbanh, CA) and a 3 DOF commercial manipulator (Marzhauser-Wetzlar, DC3-R-L, Germany) were integrated into the setup. Conductive glue (Ablebond 84-1, Ablestik, Berkeley, CA) was used in the first trials, but during the curing process at 150 °C, most of the electrical contacts were lost. Surface mount device (SMD) soldering paste (ISO Cream, EL3202, Felder Löttechnik, Germany), with small solder particles in the size range between 5 μm and 15 μm, was then considered. This paste was dispensed through a 30 gauge needle suitable for the task. The electrical connections functioned well, but the mechanical bonding was observed to be quite fragile and fractures occurred when applying a tangential force of 1–2 N on the sensor. The final choice was then the Z-axis conductive film 5552R (3M, St. Paul, MN). This tape electrically connects and mechanically bonds circuit lines with a pitch down to 100 μm through the adhesive thickness (the Z axis). Mounting the sensor using this film required further critical process steps compared to soldering and gluing, e.g., thermal ramp profile control for the tape activation, while maintaining constant normal loading conditions. However, the results have shown excellent electrical contacts (less than 1 Ω contact resistance) and reliable mechanical bonding (the sensor cannot be mechanically detached without destroying the silicon substrate).

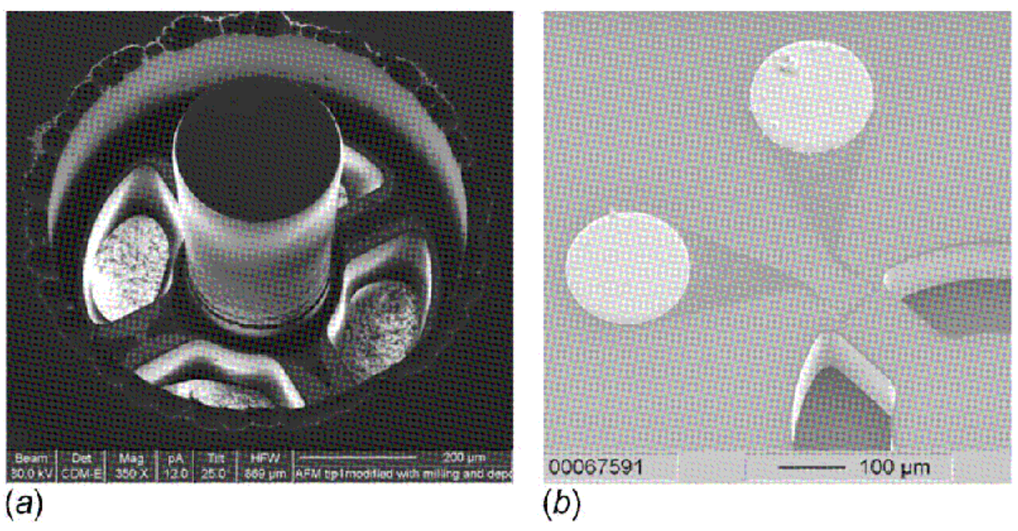

Fig. 4 (*a*) Focused ion beam image of the triaxial force sensor and (*b*) scanning electron microscope image of one piezoresistor and its two connection pads

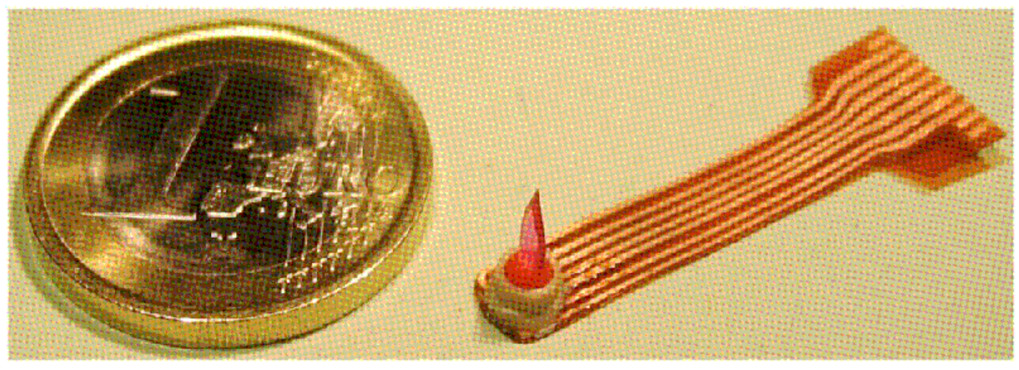

Fig. 5 The fabricated device

The second part of the assembly process began with mounting the sensor external support (fabricated in polyether ether ketone (PEEK™) by using a five-axis computer numerical control (CNC) machining center) onto the flexible circuit using a UV-light curing adhesive (ELC 4481, Electro-Lite Corp., Bethel, CT). In the next step, 10 mg of soft polyurethane (Poly 74-45, PolyTek, Humble, TX) was dispensed into the housing and the cleaned nylon ball was inserted. The amount of polyurethane, together with a tailored assembly tool, allowed us to achieve the desired gap D between the ball and the sensor tip. After polymer curing at room temperature, the blade was glued to the ball by a strong adhesive glue (M-Bond 200 Adhesive, M-Line, Raleigh, NC). A picture of the fabricated device is reported in Fig. 5.

2.3 Electronics. As described above, four piezoresistors (ranging from 800 Ω to 1 kΩ) were used to measure the sensor tip deflection and then the applied force. Each piezoresistor variation was measured in a "quarter-Wheatstone bridge" configuration. To amplify the bridge signals to a level between −10 V and 10 V, four instrumentation amplifiers (AD620, Analog Devices, Norwood, MA), with an amplification factor of 430, were used. No analog filtering was applied. A data acquisition card (DAQ-6062E, National Instruments, Austin, TX) allowed digitizing of the four signals. The software platform was Windows XP and National Instruments LABVIEW 7.0.

3 Calibration

The test bench used to characterize the knife had similar features as that reported in a previous work [22], where it had been used for the bare silicon sensor characterization. The experimental apparatus used in this work encompassed a different support, suitable to maintain the device in a fixed position during loading tests.

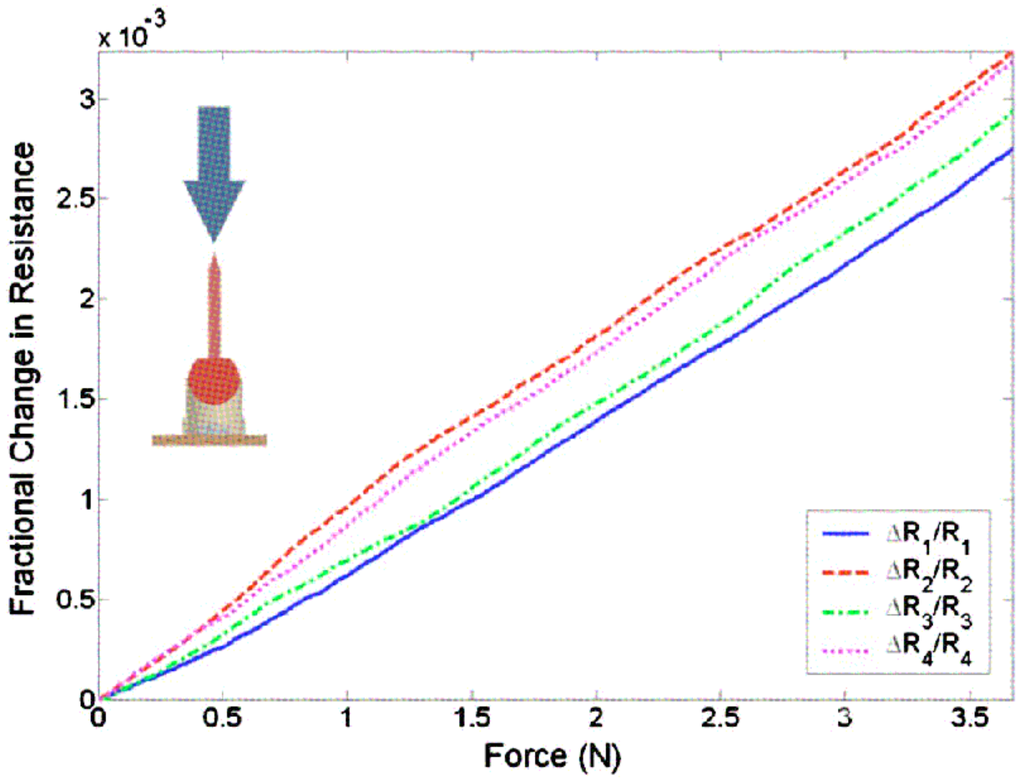

Fig. 6 Sensor response to normal loading

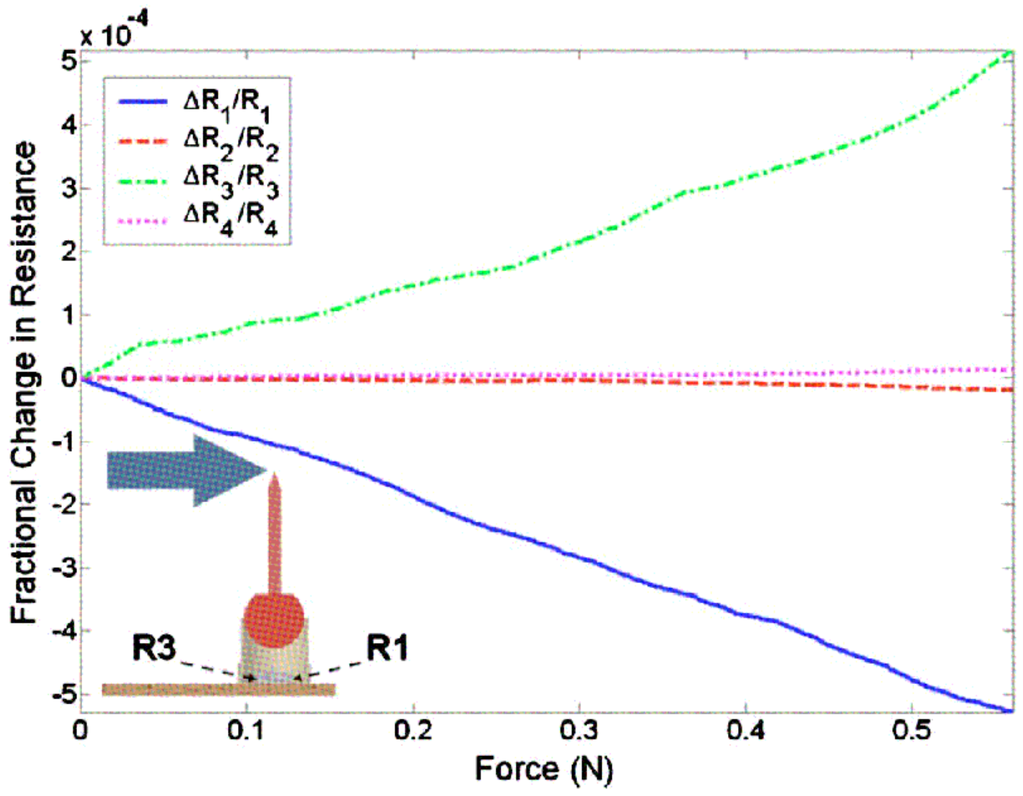

Fig. 7 Sensor response to tangential loading along $R_3 \rightarrow R_1$ direction

In the test procedure, a six component load cell, mechanically connected to a motorized nanotranslator, applied a controlled load to the blade.

Three loading schemes are needed for a proper calibration of the device:

- normal loading (Z axis)
- tangential loading along the $R_3 \rightarrow R_1$ direction (X axis) and
- tangential loading along the $R_2 \rightarrow R_4$ direction (Y axis)

The sensor outputs along these three loading configurations are linearly independent and allow, in the case of linearity, to build a calibration matrix starting from the acquired data. The correct loading along the translational direction of the nanoslider is ensured by the null readings of the other components of the pushing force, which are acquired by the six component load cell. The obtained calibration matrix can be used to directly evaluate in real time the force output during cutting interventions.

3.1 Device Characterization. During normal tests, a load increasing from 0 N up to 3.6 N was applied at a translational constant speed of 35 μm s^{-1}. Sensor outputs, in terms of fractional change in resistance $\Delta R/R$ versus normal loading force, are plotted in Fig. 6. The coefficient of determination, which quantifies the linearity of the curve as it is close to 1, was found to be 0.99 for all the piezoresistor outputs.

In order to characterize the dynamical behavior of the device, a step response test was performed. Therefore, a 5 N normal load was applied to the sensor and removed instantaneously. The signal rise time t_{95}, defined as the time required to reach 95% of the steady value of force, was found to be smaller than 4 ms, corresponding to a frequency of 250 Hz. So, the range of frequencies relevant for haptic feedback and tissue mechanical property measurement (i.e., from dc to hundreds of hertz [25]) is covered.

The sensor outputs for an applied tangential load along the X axis are plotted in Fig. 7. In this configuration, the sphere transmits the applied force to the polyurethane filling and then to the force sensor; in this way, R_3 and R_1 exhibit an opposite behavior, while R_2 and R_4 are not significantly influenced. The same applies to the results of a pure tangential loading along the Y axis.

The standard deviation of the calibration data, evaluated on 20 trials, was 1.4% of the signal full scale range. Due to the lack of a fifth dummy piezoresistor on the sensor, a real temperature compensation, like the one achievable using a "half-Wheatstone bridge" configuration, was not possible. On a symmetrically fabricated device, a temperature change should result in the same ΔR of all piezoresistors and should therefore appear in the calculated forces only as a normal force variation, while tangential forces should not be affected. Typical normal force change due to temperature was about 0.07 N/°C. However, since the device is designed to work in a surgical environment, it will be used almost at a constant temperature of 37°C, that is, the human body temperature; thus, thermal drift should not be a major problem.

Maximum loading force ranges were experimentally evaluated. Regarding normal loadings, the device overloading limit increased from 3 N of the bare silicon sensor up to 30 N, thanks to the polyurethane filling that absorbed much of the applied force as strain energy. While for tangential forces, the detachment of the nylon ball from the polyurethane filling occurred at 2.5 N. In order to prevent this situation, a cap with a slot for the blade can be designed in order to stop the lateral blade movement before the critical threshold is reached. Normal force resolution, limited by sensor noise performances, was about 100 mN for the unfiltered signal. Considering a force range between 0 N and 30 N, the resolution in terms of bits was 8.2. As regards tangential forces, the lowest force that could be resolved was 40 mN; thus, the resolution in terms of bits was 7 over a range that spanned from −2.5 N to 2.5 N.

3.2 Calibration Matrix. Once the linearity of the device was assessed, a linear transformation from the four values of fractional changes in resistance (vector $\overline{\Delta \mathbf{R}/\mathbf{R}}$) to the values of the three components of the force (vector $\bar{\mathbf{F}}$) could be used. The linear transformation $\mathbf{K}$ applied [22] is the following:

$$\bar{\mathbf{F}} = \mathbf{K}\frac{\overline{\Delta \mathbf{R}}}{\mathbf{R}} \tag{1}$$

The $\mathbf{K}$ matrix for the proposed device resulted in the following:

$$\mathbf{K} = \begin{pmatrix} -589 & 0 & 537 & 0 \\ 0 & 485 & 0 & -518 \\ 270 & 339 & 305 & 297 \end{pmatrix} \text{N} \tag{2}$$

and the experimental sensitivity matrix $\mathbf{S}_E$, which is the Moore–Penrose pseudoinverse of matrix $\mathbf{K}$, was

$$\mathbf{S_E} = \begin{pmatrix} -9.4 & 0 & 7.6 \\ 0 & 9.3 & 8.7 \\ 8.3 & 0 & 8 \\ 0 & -10.6 & 8.6 \end{pmatrix} \times 10^{-4}\ \text{N}^{-1} \tag{3}$$

Thus, the sensitivities [22] were

$$S_x = 9.4 \times 10^{-4}\ \text{N}^{-1}$$

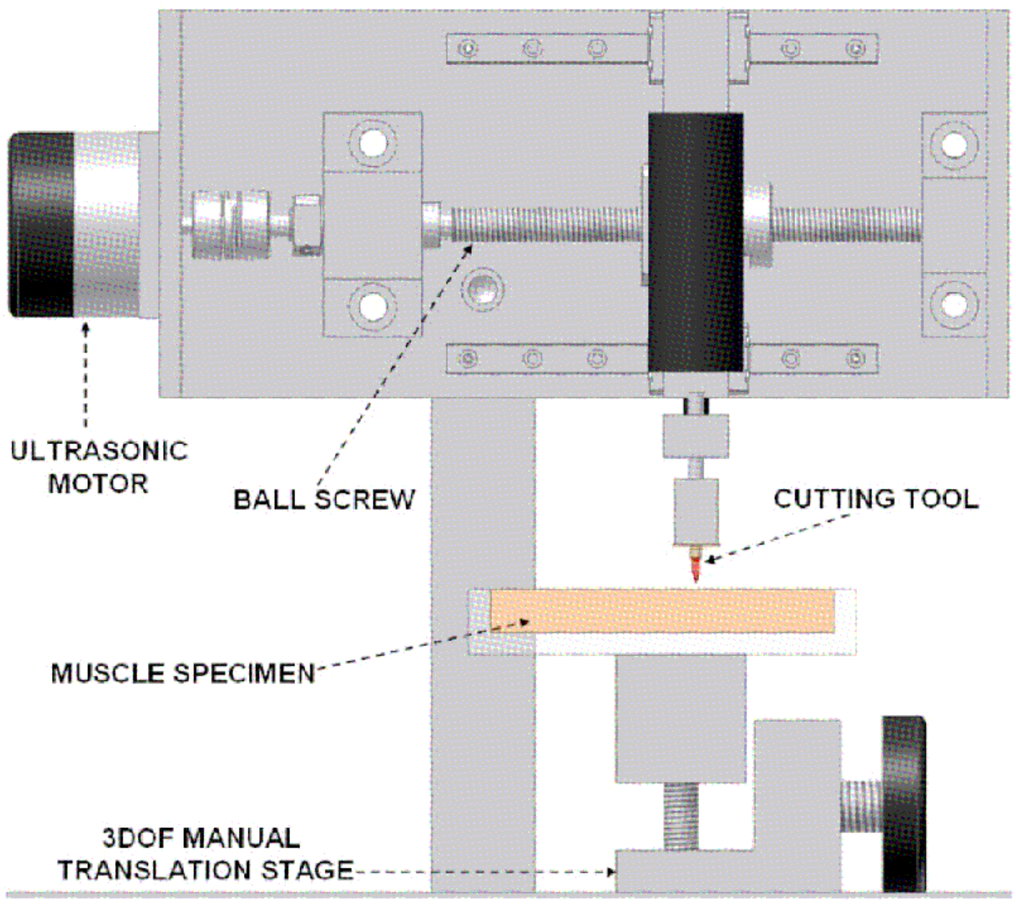

Fig. 8 Schematic view of the experimental setup for muscular tissue cutting

$$S_y = 10.6 \times 10^{-4}\ \mathrm{N}^{-1}$$

$$S_z = 8.7 \times 10^{-4}\ \mathrm{N}^{-1}$$

4 Muscle Cutting Experiments

Preliminary experiments on muscle cutting were performed in order to validate the capabilities of the proposed device to supply real time force feedback in robotic assisted surgery tasks.

4.1 Experimental Setup Description. The experimental setup is sketched in Fig. 8. It consisted of a computer controlled cutting subsystem mounted on an x-y-z manual micrometric translation stage, where an ex vivo pig muscular tissue specimen was constrained on a plastic sample holder.

The cutting device was mounted on a ball screw slider driven by an ultrasonic motor with an integrated incremental encoder (USR-30-ED-CONT, Fukoku Co., Japan). The maximum displacement the slider could achieve was 100 mm with a selectable speed that ranged from 0.01 mm/s to 5.0 mm/s. A proportional derivative (PD) controller was implemented in order to enable precise movement of the slider during cutting tasks. The design and construction of the cutting assembly ensured that the system was sufficiently rigid and had minimal backlash, so that the forces recorded by the sensor were those obtained just by the tissue cutting action.

A rectangular flat ex vivo pig muscle specimen ($80 \times 80 \times 10\ \mathrm{mm}^3$) was glued with cyanoacrylate adhesive onto a plastic frame in order to obtain a constrained boundary to simulate the physiological environment of muscles. Saline solution was sprayed on the specimen once every 5 min in order to maintain physiological conditions and to avoid drying. Muscular tissue cutting was tested in the longitudinal direction by orienting the slider movement along the muscular fibers. During each cutting test, force signals from the device were acquired during a slider movement of 10 mm at a translational constant speed of 1 mm/s. In order to have repeatable results, a preload of 100 mN was imposed as a starting condition. Ten trials were performed in order to validate the results. For each cutting trial, the achieved cut dimensions were estimated using a 2.1 megapixel digital optical microscope (VH-8000, Keyence, Japan).

4.2 Results. The three components of force recorded by the sensor during a cutting task of muscular fibers are plotted in Fig. 9. The cutting movement direction was oriented along the y axis of the sensor. An effective cut of 8.87 mm was achieved. From the experimental data, it was possible to observe a typical cutting path [18], formed by a repeated sequence of localized tissue deformation (indicated as Phase 1 in Fig. 9), followed by localized tissue fractures (indicated as Phase 2 in Fig. 9), that determine a drop in the force signal. F_y can be used to give the surgeon feedback about which phase of the cutting cycle is taking place (in this particular cutting mode, where the blade travels parallel to the material plane). F_y was not the only significative component of the force signal. From Fig. 9, it is clearly evident that F_x and F_z cannot be neglected. This can be explained in the following way: During the buildup to cut initiation (Phase 1), the F_x arises due to the warping of the tissue out of plane—it is possible to assume that this warping is not symmetrical about the blade and this force imbalance causes a moment couple. F_z could also be explained in terms of tissue warpage: Again, during the buildup to cutting initiation (Phase 1), the warpage of the tissue out of plane causes a downward force due to friction on the blade. It can be noted that the maximum values of F_x and F_z coincide with the point of cut initiation, where tissue warpage is maximum. As previously reported, the actual cutting length was shorter than the performed displacement. This is because after sliding was stopped, the minimum force to continue cutting was not maintained.

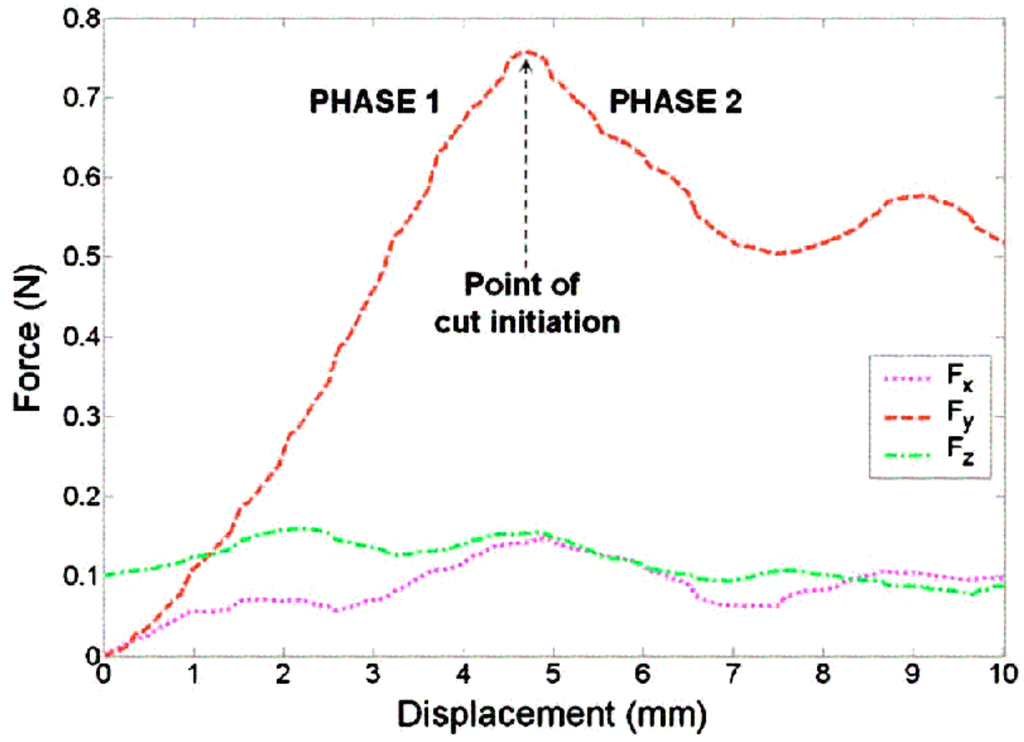

Fig. 9 Sensor output during cutting test

5 Conclusions

In the present paper, a novel triaxial force sensorized tool for endoluminal interventions and MIRS has been presented. Its small dimensions (outer diameter less than 3 mm) make this device suitable to be inserted through a 9 French catheter guide into the human body. A normal force resolution is 8.2 bits over a force range between 0 N and 30 N, while tangential force resolution is 7 bits over a range of 5 N. The device proposed in this work is intended for tissue cutting tasks. However, if the final part of the tool, i.e., the ruby knife, is replaced with a different kind of shape, then different clinical applications can be addressed (i.e., tissue palpation). Force signals with frequencies up to 250 Hz can successfully be detected, enabling haptic feedback and tissue mechanical property investigation. A calibration matrix has been evaluated for the proposed force sensor, allowing a real time force monitoring. This has been applied in a muscular tissue cutting experiment, where all the three force components have been recorded during the knife movement. Thanks to these information, a surgeon can drive a manipulator during MIRS operations taking advantage of real time triaxial force feedback.

All the device components are biocompatible; however, sterilization issues must still be addressed in future work. Safety re-

lated to electrical wiring must also be considered in the future. A strategy that can be easily adopted to improve electric safety is using an isolation amplifier (e.g., AD208 from Analog Devices) instead of a normal instrumentation amplifier. Moreover, further improvements of the system can be the addition of a dummy piezoresistor that would enable temperature compensation, and the introduction of a half bridge configuration in the signal acquisition board, allowing an increase of 1 bit of resolution for each force direction. Most future work will be oriented toward the integration of the sensing device into a robotic aided surgery system in order to have triaxial force feedback in robotic guided endoluminal interventions.

Acknowledgment

The work described in this paper was supported by the Fondazione Cassa di Risparmio di Pisa, in the framework of the "microSURF" project for the development of innovative tools and techniques in fetal surgery, and by the ASSEMIC project, a Marie Curie Research and Training Network (MRTN-CT-2003-504826). The authors would also like to thank the Italian Ministry of Foreign Affairs, General Directorate for Cultural Promotion and Cooperation for its support in the establishment of the RoboCasa laboratory. The silicon force sensor realization has been supported by the European Commissions Improving Human Potential (IHP) Program in collaboration with the Institut für Mikrotechnik Mainz (IMM), Germany. Aspecial mention to C. Filippeschi for his continuous and invaluable help.

References

[1] Rebello, K., 2004, "Applications of MEMS in Surgery," Proc. IEEE, **92**(1), pp. 43–55.
[2] Dario, P., Hannaford, B., and Menciassi, A., 2003, "Smart Surgical Tools and Augmenting Devices," IEEE Trans. Rob. Autom., **19**(5), pp. 782–792.
[3] Strandman, C., Smith, L., Tenerez, L., and Hök, B., 1997, "A Production Process of Silicon Sensor Elements for a Fibre-Optic Pressure Sensor," Sens. Actuators, A, **63**(1), pp. 69–74.
[4] Verimetra, Inc., Pittsburgh, PA, URL http://www.verimetra.com
[5] Millar Instruments, Inc., Houston, TX, USA. URL http://www.millarinstruments. com
[6] Ito, M., Yamamoto, E., Hashimoto, S., Komazaki, I., Miyajima, H., Shinohara, S., and Yanagisawa, K., 1995, "Compound-Cavity Tactile Sensor Using Surface-Emitting Laser for Endoscope/Catheter Tips," *Proceedings of the Sixth International Symposium on Micro Machine and Human Science (MHS'95)*, pp. 83–88.
[7] Tanimoto, M., Arai, F., Fukuda, T., Iwata, H., Itoigawa, K., Gotoh, Y., Hashimoto, M., and Negoro, M., 1998, "Micro Force Sensor for Intravascular Neurosurgery and In Vivo Experiment," *Proceedings of the IEEE International Workshop on Microelectromechanical Systems (MEMS'98)*, pp. 504–509.
[8] Mineta, T., Mitsui, T., Watanabe, Y., Kobayashi, S., Haga, Y., and Esashi, M., 2002, "An Active Guide Wire With Shape Memory Alloy Bending Actuator Fabricated by Room Temperature Process," Sens. Actuators, A, **97–98**, pp. 632–637.
[9] Ohta, R., 2001, "Results of R&D on Catheter-Type Micromachine," *Proceedings of the 2001 International Symposium on Micromechatronics and Human Science (MHS'01)*, pp. 5–12.
[10] Ortmaier, T., 2002, "Motion Compensation in Minimally Invasive Robotic Surgery," Ph.D. thesis, Technische Universität München, Munich, Germany.
[11] Cepolina, F., and Michelini, R. C., 2004, "Review of Robotic Fixtures for Low-Invasiveness Surgery," Int. J. Med. Rob. Comput. Assist. Surg., **1**(1), pp. 43–63.
[12] Wagner, C. R., Stylopoulos, N., and Howe, R. D., 2002, "The Role of Force Feedback in Surgery: Analysis of Blunt Dissection," *Proceedings of the IEEE Tenth Symposium on Haptic Interfaces for Virtual Environment and Teleoperator Systems*, pp. 73–79.
[13] Eisinberg, A., Izzo, I., Valdastri, P., Menciassi, A., and Dario, P., 2004, "A Teleoperated SDM-Based Microinstrument for Vessel Recognition During MIS," *Proceedings of the IEEE Mechatronics and Robotics (MechRob'04)*, Vol. 3, pp. 1067–1071.
[14] Kern, T. A., and Werthschtzky, R., 2005, "Design of a Haptic Display for Catheterization," *Proceedings of the IEEE First Joint Eurohaptics Conference and Symposium on Haptic Interfaces for Virtual Environment and Teleoperator Systems (WHC'05)*, pp. 477–478.
[15] Seibold, U., Kübler, B., and Hirzinger, G., 2005, "Prototype of Instrument for Minimally Invasive Surgery With 6-Axis Force Sensing Capability," *Proceedings of the IEEE International Conference on Robotic and Automation (ICRA'05)*, pp. 498–503.
[16] Peirs, J., Clijnen, J., Reynaerts, D., Brussel, H. V., Herijgers, P., Corteville, B., and Boone, S., 2004, "A Micro Optical Force Sensor for Force Feedback During Minimally Invasive Robotic Surgery," Sens. Actuators, A, **115**, pp. 279–284.
[17] Berkelman, P. J., Whitcomb, L. L., Taylor, R. H., and Jensen, P., 2003, "A Miniature Microsurgical Instrument Tip Force Sensor for Enhanced Force Feedback During Robot-Assisted Manipulation," IEEE Trans. Rob. Autom., **19**(5), pp. 917–922.
[18] Chanthasopeephan, T., Desai, J., and Lau, A., 2003, "Measuring Forces in Liver Cutting: New Equipment and Experimental Results," Ann. Biomed. Eng., **31**(11), pp. 1372–1382.
[19] Chanthasopeephan, T., Desai, J. P., and Lau, A. C. W., 2004, "Deformation Resistance in Soft Tissue Cutting: A Parametric Study," *Proceedings of the 12th International Symposium on Haptic Interfaces for Virtual Environment and Teleoperator Systems (HAPTICS'04)*, pp. 323–330.
[20] Bielser, D., and Gross, M. H., 2000, "Interactive Simulation of Surgical Cuts," *Proceedings of the Computer Graphics and Applications (CGA'00)*, pp. 116–442.
[21] Beccai, L., Roccella, S., Arena, A., Valvo, F., Valdastri, P., Menciassi, A., Carrozza, M. C., and Dario, P., 2005, "Design and Fabrication of a Hybrid Silicon Three-Axial Force Sensor for Biomechanical Applications," Sens. Actuators, A, **120**, pp. 370–382.
[22] Valdastri, P., Roccella, S., Beccai, L., Cattin, E., Menciassi, A., Carrozza, M. C., and Dario, P., 2005, "Characterization of a Novel Hybrid Silicon Three-Axial Force Sensor," Sens. Actuators, A, **123–124C**, pp. 249–257.
[23] Valdastri, P., Harada, K., Menciassi, A., Beccai, L., Stefanini, C., Fujie, M., and Dario, P., 2006, "Integration of a Miniaturised Triaxial Force Sensor in a Minimally Invasive Surgical Tool," IEEE Trans. Biomed. Eng., **53**(11), pp. 2397–2400.
[24] Basdogan, C., De, S., Kim, J., Muniyandi, M., Kim, H., and Srinivasan, M. A., 2004, "Haptics in Minimally Invasive Surgical Simulation and Training," IEEE Comput. Graphics Appl., **24**(2), pp. 56–64.
[25] Ottensmeyer, M. P., and Salisbury, J. K., 2001, "In Vivo Data Acquisition Instrument for Solid Organ Mechanical Property Measurement," *Proceedings of the MICCAI*, pp. 975–982.